

Synthesis and X-ray Structures of Tin(IV) and Lead(II) Complexes with Heterocyclic Thiones

Antonio Sousa-Pedrares,^{*,[a]} María I. Casanova,^[a] José A. García-Vázquez,^[a] María L. Durán,^[a] Jaime Romero,^[a] Antonio Sousa,^{*,[a]} Jack Silver,^[b] and Philip J. Titler^[b]

Keywords: Tin / Lead / N ligands / S ligands / Heterocycles

Tin(IV) and lead(II) complexes of 3-(trifluoromethyl)pyridine-2-thione (3-CF₃-pySH) and 5-(trifluoromethyl)pyridine-2-thione (5-CF₃-pySH) have been synthesised. The compounds [Sn(3-CF₃-pyS)₄] (1), [Sn(5-CF₃-pyS)₄] (2), [Pb(3-CF₃-pyS)₂] (3), and [Pb(5-CF₃-pyS)₂] (4) were obtained by addition of the appropriate ligand to a methanol solution of tin(II) chloride or lead acetate in the presence of triethylamine. The complex [Sn(5-CF₃-pyS)₄] was also prepared by electrochemical oxidation of a tin anode in a cell containing an acetonitrile solution of the ligand 5-(trifluoromethyl)pyridine-2-thione. The X-ray crystal structure of [Sn(3-CF₃-pyS)₄] reveals a dodecahedral coordination geometry around Sn^{IV}, with the four

thionate ligands acting in a bidentate (N,S) manner. [Sn(5-CF₃-pyS)₄] also consists of monomeric neutral molecules with the tin(IV) atom in an octahedral geometry with two bidentate (N,S) ligands and two monodentate S ligands. The molecular structure of [Pb(3-CF₃-pyS)₂] shows the metal in a five-coordinate geometry with the stereochemically active lead(II) lone pair in an equatorial position of a trigonal bipyramid. Spectroscopic data for the complexes (IR, NMR, FAB, and Mössbauer spectra) are discussed and related to the structural information.

(© Wiley-VCH Verlag GmbH & Co. KGaA, 69451 Weinheim, Germany, 2003)

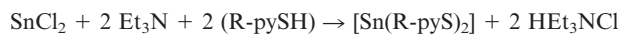
Introduction

Much of the interest in metal-sulfur chemistry results from the potential relevance of the resulting compounds to active sites in metalloenzymes and also to their ability to adopt various nuclearities of significant structural complexity.^[1–3] However, in comparison with the coordination chemistry of transition metals, the chemistry of the main group metals with sulfur ligands remains much less developed.^[4] In many cases, the interaction of toxic metals with biological systems involves bonding of the metal to the sulfhydryl groups present in enzymes. Hence, an insight into the chemistry of main group thiolate compounds is important in terms of understanding the aforementioned interaction and for the design of detoxifying agents.^[5,6] The generally poor solubility of group 14 metal/thiolate compounds makes it difficult to structurally characterise these systems and, for this reason, there is a lack of compounds whose structures have been determined by X-ray diffraction. Zubietta has determined the structures of [Sn(2-SC₃H₄N)₄]^[7] and [Sn(2-SC₃H₄N-3-SiMe₃)₄].^[8] Curiously, while [Sn(2-SC₃H₄N)₄] has a distorted octahedral structure, the structure of [Sn(2-SC₃H₄N-3-SiMe₃)₄] is dodecahedral. This suggests that the nature and location of the substituents in the

heterocyclic ring are important in determining the structure of the compound isolated. As a result of our continued interest in the coordination chemistry of thionate ligands, we decided to study the influence of the nature and location of substituents in the heterocyclic ring on the structure of the corresponding complexes. In particular, the work described here encompasses the synthesis and characterisation of tin(IV) and lead(II) complexes with 3-(trifluoromethyl)- and 5-(trifluoromethyl)pyridine-2-thionato ligands.

Results and Discussion

The reactions of 3-(trifluoromethyl)- and 5-(trifluoromethyl)pyridine-2-thione with SnCl₂ in methanol in the presence of triethylamine produce compounds whose microanalytical data correspond to SnL₄. On going from the tin precursor to the product, the metal atom is oxidised and so one possible reaction mechanism involves the formation of an initial tin(II) compound, which is subsequently oxidised in solution to tin(IV) in accordance with the following equations:

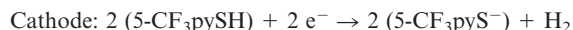


It is well-known that the electrochemical procedure for the synthesis of metal complexes produces compounds in which the metal is in a low oxidation state. For this reason,

^[a] Departamento de Química Inorgánica, Universidad de Santiago de Compostela, 15782 Santiago de Compostela, Spain

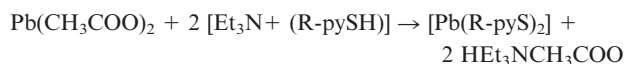
^[b] School of Chemical and Life Sciences, University of Greenwich, Wellington St, Woolwich, London, SE18 6PF, UK

we tried to ascertain whether tin(II) compounds with these ligands could be obtained using such a procedure. With this aim in mind, a solution of 5-(trifluoromethyl)pyridine-2-thione in acetonitrile was electrolysed using a tin plate as the anode. Once more, the microanalytical data and the X-ray structure (*vide infra*) for the resulting compound were consistent with the composition $[\text{Sn}(\text{5-CF}_3\text{-pyS})_4]$. The electrochemical process has an efficiency value near to $0.5 \text{ mol}\cdot\text{F}^{-1}$ ($E_f = 0.49$). This means that the anode oxidation leads initially to a tin(II) species, which is then further oxidised to $[\text{SnL}_4]$ in accordance with the following reaction sequence:



This behaviour has been observed in the synthesis of other Sn^{IV} complexes by electrochemical procedures.^[9]

The lead(II) complexes were obtained in reasonable yields by stirring the corresponding ligand and lead acetate in solution in methanol in the presence of triethylamine. The formation of these lead complexes is believed to follow a similar scheme to that described above for $[\text{Sn}(3\text{-CF}_3\text{-pyS})_4]$. However, in this case, the further oxidation step does not occur and the complexes have the general formula $[\text{PbL}_2]$.



Crystallographic Studies

Structure of $[\text{Sn}(3\text{-CF}_3\text{-pyS})_4]$ (1)

Figure 1 shows the ORTEP drawing of the structure of $[\text{Sn}(3\text{-CF}_3\text{-pyS})_4]$ along with the numbering system used.

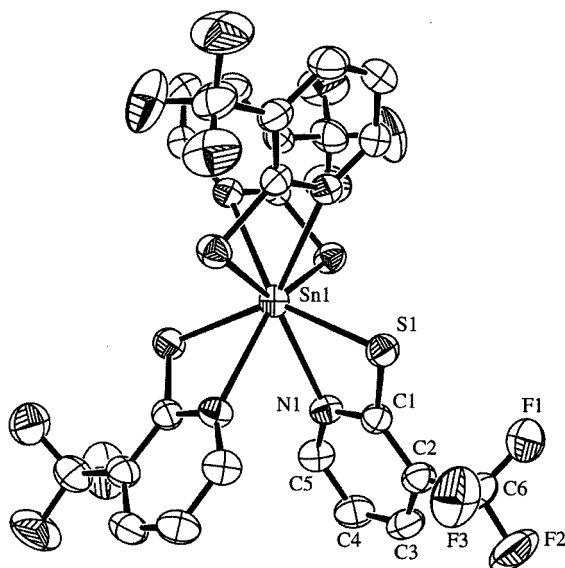


Figure 1. Molecular structure of $[\text{Sn}(3\text{-CF}_3\text{-pyS})_4]$

The relevant bond lengths and bond angles are listed in Table 1.

The structure of **1** shows the tin atom to be coordinated by four bidentate (N,S) ligands. In this arrangement the metal atom is in an eight-coordinate environment. Comparison of the parameters found with values for the corresponding ideal geometry with the same coordination number shows that, in this case, the geometry is closer to a dodecahedron than to an antiprism.

The distortion of the dodecahedral geometry with regard to the regular geometry can be understood if we consider the regular dodecahedron as being the result of the interpenetration of two regular tetrahedra (Figure 2). In the complex under discussion, the four sulfur atoms are situated at the vertices of a distorted tetrahedron and the nitrogen atoms in the vertices of another distorted tetrahedron in an alternating manner.^[10]

The main cause of distortion is the small bite of the chelate angle N–Sn–S at $61.72(5)^\circ$. Another factor that contributes to the distortion is the difference between the bond lengths Sn–N and Sn–S, which are $2.556(2)$ and $2.4935(8)$ Å, respectively. This causes the tetrahedron formed by the nitrogen atoms to be more distorted than the one formed by the sulfur atoms. In the tetrahedron formed by the sulfur atoms the values of the S–Sn–S angles are $97.322(12)$ and $138.17(3)^\circ$, while the N–Sn–N angles are $67.45(10)$ and $133.77(6)^\circ$, i.e. further from the theoretical value expected for a regular tetrahedron.

The four Sn–S bond lengths [$2.4935(8)$ Å] are not very different from those found in other tin complexes with four-membered chelate rings such as, for example, $[\text{Sn}(\text{S}_2\text{CNet}_2)_4]$ ^[11] and $[\text{Sn}(\text{S}_2\text{CNMe})_4]$,^[12] or in the complex of tin with trisilylpyridine-2-thionate, $[\text{Sn}(3\text{-Me}_3\text{Si-pyS})_4]$, where the tin atom is also eight-coordinate in a dodecahedral geometry [average value $2.496(4)$ Å].^[8]

The values of the Sn–N bond lengths are similar to those found in $[\text{Sn}(3\text{-Me}_3\text{Si-pyS})_4]$, average value $2.56(1)$ Å, but longer than the values found in $[\text{Sn}(5\text{-CF}_3\text{-pyS})_4]$, *vide infra*, where the tin atom is in a six-coordinate environment.

The pyridine rings are essentially planar and the S(1) atom lies approximately on the plane of the pyridine ring to which it is bound (maximum deviation 0.028 Å). The average S–C and C–N bond lengths [$1.768(17)$ and $1.345(16)$ Å, respectively] are intermediate between the values found in free pyridine-2-thione [$1.695(2)$ Å, $1.356(3)$ Å, respectively]^[13] and those in bis(3-*tert*-butyldimethylsilyl)-2-pyridyldisulfide^[14] [average C–S: $1.794(3)$ Å; average N–C: $1.330(5)$ Å], suggesting that the ligand is coordinating in a way that is closer to the pyridine-2-thionato form than to the thione form.

Structure of $[\text{Sn}(5\text{-CF}_3\text{-pyS})_4]$ (2)

Figure 3 shows the ORTEP drawing of the structure of $[\text{Sn}(5\text{-CF}_3\text{-pyS})_4]$ along with the numbering system used. The relevant bond lengths and bond angles are listed in Table 2.

The geometry of $[\text{Sn}(5\text{-CF}_3\text{-pyS})_4]$ can be described as a severely distorted octahedron, with the tin atom coordin-

Table 1. Selected bond lengths [\AA] and angles [$^\circ$] for complex $[\text{Sn}(\text{3-CF}_3\text{-pyS})_4]$

Sn(1)–S(1)	2.4935(8)	N(1)–C(1)	1.339(3)
Sn(1)–N(1)	2.556(2)	N(1)–C(5)	1.331(3)
S(1)–C(1)	1.742(3)		
S(1)–Sn(1)–S(1)#1 ^[a]	97.322(12)	S(1)#2–Sn(1)–N(1)#1	83.10(5)
S(1)–Sn(1)–S(1)#2	97.322(12)	S(1)#2–Sn(1)–N(1)#2	61.72(5)
S(1)–Sn(1)–S(1)#3	138.17(3)	S(1)#3–Sn(1)–N(1)	83.10(5)
S(1)#1–Sn(1)–S(1)#2	138.17(3)	S(1)#3–Sn(1)–N(1)#1	79.01(5)
S(1)#1–Sn(1)–S(1)#3	97.322(12)	S(1)#3–Sn(1)–N(1)#2	141.67(5)
S(1)#2–Sn(1)–S(1)#3	97.322(12)	N(1)–Sn(1)–N(1)#1	133.77(6)
S(1)#2–Sn(1)–N(1)#3	79.01(5)	N(1)–Sn(1)–N(1)#2	133.77(6)
S(1)#3–Sn(1)–N(1)#3	61.72(5)	N(1)–Sn(1)–N(1)#3	67.45(10)
S(1)–Sn(1)–N(1)	61.72(5)	N(1)#1–Sn(1)–N(1)#2	67.45(10)
S(1)–Sn(1)–N(1)#1	141.67(5)	N(1)#1–Sn(1)–N(1)#3	133.77(6)
S(1)–Sn(1)–N(1)#2	79.01(5)	N(1)#2–Sn(1)–N(1)#3	133.77(6)
S(1)–Sn(1)–N(1)#3	83.10(5)	C(1)–S(1)–Sn(1)	88.41(9)
S(1)#1–Sn(1)–N(1)	79.01(5)	C(1)–N(1)–C(5)	120.1(2)
S(1)#1–Sn(1)–N(1)#1	61.72(5)	C(1)–N(1)–Sn(1)	95.76(16)
S(1)#1–Sn(1)–N(1)#2	83.10(5)	C(5)–N(1)–Sn(1)	143.6(2)
S(1)#1–Sn(1)–N(1)#3	141.67(5)	N(1)–C(1)–S(1)	113.79(19)
S(1)#2–Sn(1)–N(1)	141.67(5)		

^[a] Symmetry transformations used to generate equivalent atoms. #1: $-y + 1/4, x + 1/4, -z + 1/4$, #2: $y - 1/4, -x + 1/4, -z + 1/4$, #3: $-x, -y + 1/2, z$.

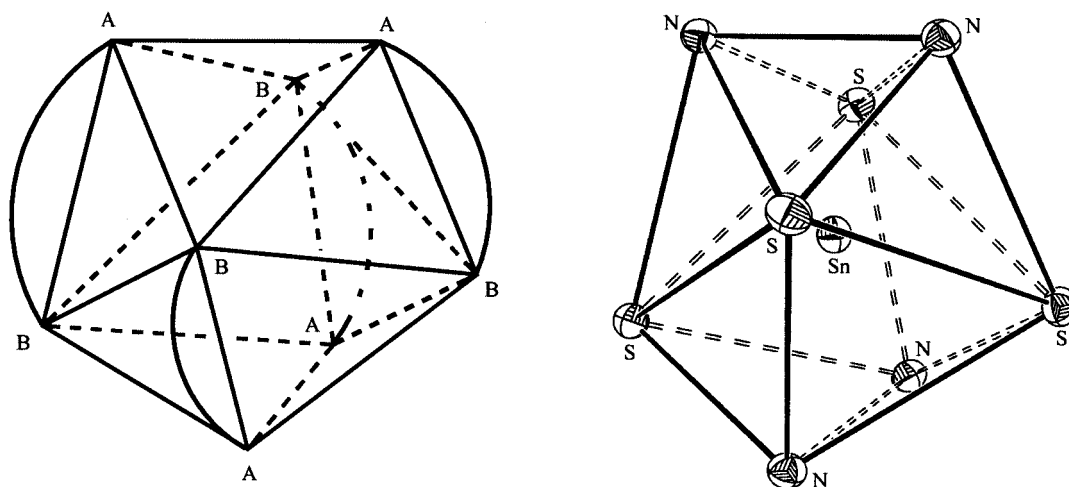


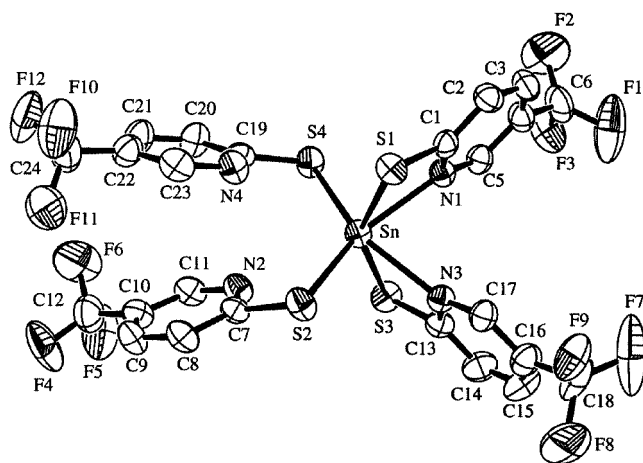
Figure 2. (left) View of the regular dodecahedral structure for a complex of the type $[\text{M}(\text{AB})_4]$; (right) view of the coordination polyhedron for the complex $[\text{Sn}(\text{3-CF}_3\text{-pyS})_4]$

ated to two monodentate S thionato ligands and two bidentate (N,S) ligands.

The arrangement of the ligands is such that the sulfur atoms of the two monodentate thionate ligands are in a *cis* disposition with respect to one another and the sulfur atoms of the two bidentate ligands are in a *trans* disposition. The main cause of the distortion is the small bite of the bidentate thionato ligands [$\text{N}–\text{Sn}–\text{S}$ angles of $64.6(9)^\circ$ and $64.9(9)^\circ$]. This situation causes the angles defined by the two *trans* atoms and the tin atom [$\text{S}(1)–\text{Sn}(1)–\text{S}(3) = 149.47(9)^\circ$, $\text{N}(1)–\text{Sn}(1)–\text{S}(2) = 149.54(5)^\circ$, and $\text{N}(3)–\text{Sn}(1)–\text{S}(4) = 148.02(5)^\circ$] to be very different from the expected values of 180° and, consequently, the angles formed by the tin and two *cis* atoms are also significantly different from 90° [$64.09(9)–122.38(4)^\circ$].

The Sn–S distances are all slightly different and depend on whether the sulfur atom is provided by the bidentate ligand [$2.4942(13)$ and $2.4921(13) \text{ \AA}$] or by the monodentate ligand [$2.4573(14)$ and $2.4618(13) \text{ \AA}$]. The longest Sn–S distance is slightly shorter than those found in the tin complex with pyridine-2-thionate $[\text{Sn}(\text{pyS})_4]^{[7]}$ [average value $2.512(2) \text{ \AA}$] but is very similar to those found in $[\text{Sn}(\text{3-CF}_3\text{-pyS})_4]$. The distances between the tin atom and the sulfur atoms of the monodentate ligands [$2.4573(14)$ and $2.4618(13) \text{ \AA}$] are slightly shorter than those of $[\text{Sn}(\text{pyS})_4]$ [average value $2.469(2) \text{ \AA}$].

The Sn–N bond lengths [$2.384(4)–2.371(4) \text{ \AA}$] are longer than the corresponding distances found in $[\text{Sn}(\text{pyS})_4]$ [$2.332(5)–2.324(5) \text{ \AA}$] but are shorter than those observed in the aforementioned eight-coordinate $[\text{Sn}(\text{3-CF}_3\text{-pyS})_4]$.

Figure 3. Molecular structure of $[\text{Sn}(\text{5-CF}_3\text{-pyS})_4]$ Table 2. Selected bond lengths [Å] and angles [°] for complex $[\text{Sn}(\text{5-CF}_3\text{-pyS})_4]$

Sn(1)–S(1)	2.4942(13)	S(4)–C(19)	1.751(5)
Sn(1)–S(2)	2.4573(14)	N(1)–C(1)	1.341(6)
Sn(1)–S(3)	2.4921(13)	N(1)–C(5)	1.335(6)
Sn(1)–S(4)	2.4618(13)	N(2)–C(7)	1.332(6)
Sn(1)–N(1)	2.384(4)	N(2)–C(11)	1.326(7)
Sn(1)–N(3)	2.371(4)	N(3)–C(13)	1.343(6)
S(1)–C(1)	1.744(5)	N(3)–C(17)	1.343(6)
S(2)–C(7)	1.754(5)	N(4)–C(19)	1.326(6)
S(3)–C(13)	1.740(5)	N(4)–C(23)	1.325(7)

S(1)–Sn(1)–S(2)	92.25(4)	C(7)–S(2)–Sn(1)	100.8(2)
S(1)–Sn(1)–S(3)	148.02(5)	C(13)–S(3)–Sn(1)	84.3(2)
S(1)–Sn(1)–S(4)	101.47(5)	C(19)–S(4)–Sn(1)	101.3(2)
S(2)–Sn(1)–S(3)	102.27(5)	C(1)–N(1)–C(5)	119.4(4)
S(2)–Sn(1)–S(4)	122.38(4)	C(1)–N(1)–Sn(1)	98.1(3)
S(3)–Sn(1)–S(4)	94.59(5)	C(5)–N(1)–Sn(1)	142.5(3)
S(1)–Sn(1)–N(1)	64.09(9)	C(7)–N(2)–C(11)	117.0(4)
S(2)–Sn(1)–N(1)	149.47(9)	C(13)–N(3)–C(17)	119.7(4)
S(3)–Sn(1)–N(1)	91.03(10)	C(13)–N(3)–Sn(1)	98.5(3)
S(4)–Sn(1)–N(1)	83.06(9)	C(17)–N(3)–Sn(1)	141.8(3)
S(1)–Sn(1)–N(3)	89.45(9)	C(19)–N(4)–C(23)	117.5(4)
S(2)–Sn(1)–N(3)	84.97(10)	N(1)–C(1)–S(1)	113.6(3)
S(3)–Sn(1)–N(3)	64.06(9)	N(2)–C(7)–S(2)	117.2(3)
S(4)–Sn(1)–N(3)	149.54(10)	N(3)–C(13)–S(3)	113.1(3)
N(1)–Sn(1)–N(3)	76.28(13)	N(4)–C(19)–S(4)	117.9(4)
C(1)–S(1)–Sn(1)	84.2(2)		

This change in Sn–N bond length could be due to a change in the coordination number from six to eight.

The C–S bond lengths of the coordinated ligand range from 1.744(5) to 1.740(5) Å with an average value of 1.742 Å for the chelating ligands and 1.754(5)–1.751(5) Å for the monodentate ligands. Both distances are similar to those found in $[\text{Sn}(\text{3-CF}_3\text{-pyS})_4]$. The C–N and C–C bond lengths of the ligands are as one would expect and do not warrant further discussion.

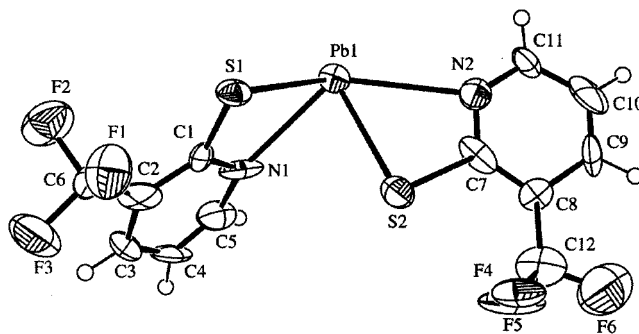
Each of the ligands is planar within experimental error, with the sulfur atoms of the bidentate ligands lying practically in the plane of the pyridine ring to which they are bound [by 0.032 Å for S(1) and 0.031 Å for S(3)]. In the case of the monodentate ligands the sulfur atoms lie out of

the pyridine plane [by 0.082 Å for S(2) and 0.095 Å for S(4)].

It is worth noting that although compounds **1** and **2** have the same composition $[\text{SnL}_4]$, their molecular structures are quite different. In the case of **1**, all of the ligands behave in a bidentate (S,N) manner and the Sn is in an eight-coordinate dodecahedral environment $[\text{SnS}_4\text{N}_4]$. Compound **2**, on the other hand, has two ligands that behave in a bidentate (S,N) way and another two that act in a monodentate S manner to give a six-coordinate octahedral geometry $[\text{SnS}_4\text{N}_2]$ around the metal atom. The remarkable feature of this arrangement is that the more crowded structure is provided by the more sterically demanding ligand, 3- CF_3 -pySH.

Structure of $[\text{Pb}(\text{3-CF}_3\text{-pyS})_2]$ (**3**)

The molecular structure of $[\text{Pb}(\text{3-CF}_3\text{-pyS})_2]$ is shown in Figure 4 together with the atom-labelling scheme. Selected bond lengths and angles are given in Table 3. The structure consists of discrete molecules without interactions between neighbours and with the lead atom coordinated by two bidentate (N,S) anionic 3-(trifluoromethyl)pyridine-2-thionato ligands. On the assumption that the lone pair on the lead atom is symmetrically placed with respect to the nitrogen and sulfur atoms, a value of 0.84 can be calculated for τ .^[15] In this situation the environment around the lead atom is best described as a pseudo-trigonal bipyramid with a 16% distortion towards a square pyramid. In this case the nitro-

Figure 4. Molecular structure of $[\text{Pb}(\text{3-CF}_3\text{-pyS})_2]$ Table 3. Selected bond lengths [Å] and angles [°] for complex $[\text{Pb}(\text{3-CF}_3\text{-pyS})_4]$

Pb(1)–S(1)	2.883(11)	S(2)–C(7)	1.81(4)
Pb(1)–S(2)	2.707(11)	N(1)–C(1)	1.42(5)
Pb(1)–N(1)	2.59(3)	N(1)–C(5)	1.33(5)
Pb(1)–N(2)	2.79(3)	N(2)–C(7)	1.23(5)
S(1)–C(1)	1.72(3)	N(2)–C(11)	1.30(5)
N(1)–Pb(1)–S(1)	57.8(7)	C(1)–N(1)–C(5)	115(4)
S(2)–Pb(1)–N(2)	55.8(8)	C(1)–N(1)–Pb(1)	102.4(19)
S(1)–Pb(1)–N(2)	125.0(9)	C(5)–N(1)–Pb(1)	143(3)
S(2)–Pb(1)–N(1)	75.3(7)	C(7)–N(2)–C(11)	121(4)
S(1)–Pb(1)–S(2)	86.4(3)	C(7)–N(2)–Pb(1)	98(3)
N(1)–Pb(1)–N(2)	129.0(10)	C(11)–N(2)–Pb(1)	136(3)
C(1)–S(1)–Pb(1)	84.2(14)	N(1)–C(1)–S(1)	115(3)
C(7)–S(2)–Pb(1)	88.3(16)	N(2)–C(7)–S(2)	115(3)

gen atoms are in axial positions and the sulfur atoms and the lone pair in equatorial positions. This geometry is highly distorted with S–Pb–S and N–Pb–N bond angles of 86.4(3)° and 129.0(10)°, respectively. The bond angles between the axial nitrogen and sulfur atoms of the equatorial plane are in the range 55.8(8)–125.0(9)°, which is significantly different from the theoretical 90° for an ideal geometry. The main sources of distortion are the small value of the bond angle of the chelate ring [N–Pb–S = 55.8(8) and 57.8(7)°] and the effect of the active lone pair of the lead atom. The values of the bond angles among axial and equatorial positions, or in other words the angles S–Pb–N between atoms corresponding to different thionato ligands, are 75.3(7) and 125.0(9)°, again significantly different to the expected value of 90°.

The Pb–S bond lengths [2.883(1) and 2.707(11) Å] are longer than the Pb–S axial distance (2.696 Å) found in bis[6-(diethylcarbamoyl)-1-hydroxy-2(1*H*)-pyridine-2-thionato-*O,S*]lead(II),^[16] but are very close to the values of 2.737(7) and 2.782(8) Å in the trinuclear complex [Pb₃(3-SiMe₃-pyS)₆].^[8]

Two different Pb–N bond lengths are observed in the compound [Pb(3-CF₃-pyS)₂]. The longest bond (2.793 Å) is similar to the distances observed for [Pb₃(3-SiMe₃-pyS)₆] [2.81(3) and 2.89(3) Å]. The other Pb–N bond length is significantly shorter at 2.59(3) Å, but is similar to the value of 2.59 Å found in other lead complexes with pyridine ligands.^[17]

The structure of this compound differs markedly from that of [Pb(3-SiMe₃-pyS)₂], which shows a trinuclear structure with pentacoordinate metal atoms: two of the metals are coordinated by two nitrogen and three sulfur atoms in a distorted trigonal pyramidal environment and the third metal by the sulfur and nitrogen atoms of the two chelating ligands in a square pyramidal arrangement with the lead atom at the apex. Note that [Pb(3-SiMe₃-pyS)₂] has the more associated structure, despite the fact that contains a SiMe₃ group, which is considerably more bulky than the CF₃ group. Hence, in these cases steric hindrance is not a factor that determines the degree of association.

The pyridine rings of the ligands are essentially planar but the sulfur atoms lie out of the plane of the pyridine ring to which they are bound [by 0.077 Å for S(1) and 0.076 Å for S(2)]. The interplanar angle between these two ligands is 65.98°. The C–S bond lengths for the two ligands are also very different [C(1)–S(1) = 1.72(3) Å and 1.81(4) Å] but the average value of 1.765(4) Å is similar to those found in the complexes described above.

Spectroscopic Data

IR Spectra

The IR spectra of the complexes do not show bands assignable to $\nu(\text{N–H})$, which in the free ligands appear at 3175 cm^{−1}. This suggests that deprotonation of the NH group has occurred during the synthesis and therefore that the ligand is coordinated in the thionato form. This conclusion is supported by the shift to smaller wavenumbers of

the strong bands for $\nu(\text{C=C})$ and $\nu(\text{C=N})$, which appear at 1604–1545 and 1570–1512 cm^{−1} in the free ligands, on going from the free ligands to the complexes. In addition, the bands attributable to the ring breathing vibration at ca. 1000 and 630 cm^{−1} and the bands due to the C–H bending vibration at ca. 770 and 750 cm^{−1} are shifted to higher frequencies with respect to the free ligand. These shifts provide evidence that the nitrogen atom is bound to the metal atom.

NMR Spectra

The ¹H NMR spectra of the complexes do not show a signal for the NH proton, which appears as a broad singlet between $\delta = 13.0$ and 14.0 ppm in the spectrum of the free ligand, thus demonstrating that in the complexes the ligands are deprotonated. The signals of all the hydrogen atoms of the pyridine ring are shifted to lower-field values in the complexes relative to the same signals in the spectra of the free ligands. The main change observed is the low-field shift of the signal due to the proton *ortho* to the nitrogen atom of the pyridine ring ($\delta = 9.18$ –8.14 ppm), demonstrating the coordination of the ligands to the metal atoms through the pyridine nitrogen.

It should be noted that in the case of [Sn(5-CF₃-pyS)₄], if the structure observed in the solid state is maintained in solution, two different types of ligands should be observed in the NMR spectrum. In particular, two different signals should be observed in the ¹H NMR spectrum for the proton *ortho* to the pyridine rings, two signals for C² and C⁶ in the ¹³C NMR spectrum, and two signals in the ¹⁹F NMR spectrum. However, at room temperature only one signal is observed for each of these nuclei. This shows that the compound has a fluxional behaviour in solution. In order to investigate this possibility further, the spectrum was acquired at different temperatures down to −55 °C. Unfortunately, the spectrum does not change, showing that the fluxional exchange is too fast even at the lowest temperature compatible with the solvent used.

It is well-known that ¹¹⁹Sn NMR spectroscopy is very sensitive to changes in the coordination number of tin(IV)^[7] and can be used to determine the denticity of the ligands. The ¹¹⁹Sn NMR spectrum of **2** in CD₃Cl at room temperature consists of a singlet at $\delta_{\text{Sn}} = -500.5$ ppm. This value is similar to that of the hexacoordinate tin(IV) complex [Sn(pyS)₄], which also has a distorted octahedral [SnN₂S₄] environment with two ligands acting as monodentate S-bonded systems and another two as bidentate N,S bonded ligands.^[7] The ¹¹⁹Sn NMR spectrum of complex **1** shows a signal at $\delta_{\text{Sn}} = -662.6$ ppm. The shift observed with respect to **2** is consistent with an increase in the coordination number from six to eight on going from **2** to **1**, and shows that the solid-state environment of **1** is maintained in solution.

Mass Spectra

The tin and lead complexes were also characterised by mass spectrometry using the positive ion FAB technique (*m/z*) in 3-nitrobenzyl alcohol (NBA) as matrix. The FAB spectrum of [Sn(3-CF₃-pyS)₄] shows the molecular ion

at $m/z = 831$, as well as peaks due to the fragments $[\text{Sn}(\text{3-CF}_3\text{-pyS})_3]$, $[\text{Sn}(\text{3-CF}_3\text{-pyS})_2]$, and $[\text{Sn}(\text{3-CF}_3\text{-pyS})]$ at $m/z = 654$, 475, and 298, produced by the loss of one, two, and three thionate ligands, respectively. The spectrum of the compound $[\text{Sn}(\text{5-CF}_3\text{-pyS})_4]$ does not show the molecular ion peak, but does show peaks associated with $[\text{Sn}(\text{5-CF}_3\text{-pyS})_3]$, $[\text{Sn}(\text{5-CF}_3\text{-pyS})_2]$, and $[\text{Sn}(\text{5-CF}_3\text{-pyS})]$ at $m/z = 654$ (100%), 475, and 298, respectively.

The FAB mass spectra of the lead compounds, $[\text{Pb}(\text{RpyS})_2]$ show, in all cases, the molecular ion peak at $m/z = 563$ along with a peak at $m/z = 385$, which is associated with $[\text{Pb}(\text{RpyS})]$ formed by loss of one thionate ligand. This evidence, together with the fact that the ^{19}F NMR spectra of both compounds are very similar, shows that $[\text{Pb}(\text{5-CF}_3\text{-pyS})_2]$ is a monomer with a structure similar to that of $[\text{Pb}(\text{3-CF}_3\text{-pyS})_2]$.

Mössbauer Spectroscopy

The ^{119}Sn Mössbauer data for compounds **1** and **2** appear in Table 4.

Table 4. ^{119}Sn Mössbauer Spectroscopic data recorded at 78 K

Compound ^[a]	δ [$\text{mm}\cdot\text{s}^{-1}$]	ΔE_Q [$\text{mm}\cdot\text{s}^{-1}$]	Γ ^[a] [$\text{mm}\cdot\text{s}^{-1}$]
$[\text{Sn}(\text{3-CF}_3\text{-pyS})_4]$ (1)	0.93(1)	1.12(2)	1.16(3)
$[\text{Sn}(\text{5-CF}_3\text{-pyS})_4]$ (2)	0.98(1)	0.84(3)	1.14(6)

^[a] Full width at half-mean height.

The *isomer shift* (δ) values are dependant on the *s*-electron density at the tin nucleus relative to a reference standard (BaSnO_3). As the *s*-electron density at the tin nucleus is measured relative to that in the valence shell of the atom, then factors that affect the latter must also affect the former. Therefore *p*-electron shielding and the polarity of the tin-ligand bonds,^[18,19] together with their number, will affect δ .^[20]

Clearly compound **1** has the smallest δ value, in keeping with the fact that it has eight ligands and these are relatively far from the Sn atom compared to those of compound **2**. Hence we would expect the environment to be “more ionic” and hence less *s*-electron density on the tin atom. The coordination number or stereochemistry at the tin also affects the δ value. When the coordination number of the tin atom increases, the concomitant increased involvement of the metal *5d* orbitals for bonding leads to a reduction in the *5s* electron density at the tin nucleus.^[20,21]

The *quadrupole splitting* (ΔE_Q) arises from the interaction of the tin nucleus with the electric field gradient (EFG). If the tin atom has a perfectly symmetrical electronic environment (“cubic”) then there is no EFG and only a single line is observed in the Mössbauer spectrum (as for SnMe_4).^[21] Any deviation from a cubic electronic environment results in a doublet spectrum. As the EFG is the second derivative of the potential, its magnitude is inversely related to the cube of the distance of the charge from the nucleus. Therefore electron density on the Sn atom makes a larger contribution to ΔE_Q than that in the tin-ligand bonds. These lat-

ter are more important than charges on neighbouring atoms or ions.

Compound **1** has a ΔE_Q value of $1.12(2) \text{ mm}\cdot\text{s}^{-1}$ which is larger than that obtained for compound **2**. This means that the EFG in **1** is larger than that of **2**. This is in keeping with the distortion of the dodecahedral arrangement found in the structure of **1** and most probably arises from the imbalance of the electron density in the tin–ligand bonds, though the different polarity induced by the nitrogen and sulfur ligands must also play a role.

Compound **2** has a ΔE_Q value of $0.84(3) \text{ mm}\cdot\text{s}^{-1}$ which, although small, is substantial for an octahedral electronic environment. A perfect octahedral site would be expected to have zero splitting in a cubic structure. In this case it is in keeping with a highly distorted octahedral environment and is thus very compatible with the structure of compound **2**. It should be noted that these two Mössbauer spectra have low recoil-free fractions and hence were collected at 78 K only, whereas the crystal structures of **1** and **2** were recorded at room temperature. However at the very least it is shown here that the structures do not become symmetrical upon cooling to 78 K, and that in fact the Mössbauer spectra recorded at 78 K may reflect the room temperature structures.

Conclusions

The results discussed in this paper show that the structures of complexes of tin(IV) and lead(II) with derivatives of pyridine-2-thione depend on the nature and location of the substituents on the heterocyclic ring. Indeed, while $[\text{Sn}(\text{5-CF}_3\text{-pyS})_4]$ has an $[\text{SnN}_2\text{S}_4]$ octahedral geometry around the metal atom, the structure of $[\text{Sn}(\text{3-CF}_3\text{-pyS})_4]$ shows the tin atom in an $[\text{SnN}_4\text{S}_4]$ dodecahedral environment. On the other hand, while $[\text{Pb}(\text{3-CF}_3\text{-pyS})_2]$ and $[\text{Pb}(\text{5-CF}_3\text{-pyS})_2]$ are mononuclear compounds with the lead atom in a trigonal bipyramidal environment, $[\text{Pb}(\text{3-SiMe}_3\text{-pyS})_2]$ has a trimeric molecular structure. It appears that the factor responsible for this different behaviour is not of a steric nature, as the most sterically demanding ligands produce the structures with the higher coordination numbers. Further work is required to clarify this interesting phenomenon.

Experimental Section

Microanalysis were performed using a Carlo–Erba EA1108 microanalyser. Infrared spectra were recorded as compressed KBr discs by using an IR-FT Mattson model CYGNUS-100. Electron impact (EI) and fast atom bombardment (FAB) mass spectra were recorded on Hewlett–Packard HP5988A and Micromass Autospec spectrometers, respectively, with 3-nitrobenzyl alcohol as the matrix for the FAB spectra. ^1H and ^{13}C NMR spectra were recorded on a Bruker AMX300 using CDCl_3 as solvent and TMS as internal reference. ^{119}Sn NMR spectra were recorded on a Bruker AMX500 spectrometer using CDCl_3 as solvent and saturated SnMe_4 as a secondary reference. ^{19}F NMR spectra were recorded on a Bruker AMX300 spectrometer and referenced to CFCl_3 . All Mössbauer

spectra were recorded at 78 K, with a ^{119}mSn 23.875 keV γ source (370MBq, 10 mCi CaSnO_3 matrix, Wissel GmbH) mounted on the previously reported experimental setup.^[22] All thiones and metal salts were commercial products and were used without further purification.

Preparations

All the complexes were prepared by reaction of a methanolic solution of the corresponding thione and triethylamine with a solution of the tin(II) or lead(II) salts in the same solvent. Tetrakis[5-(trifluoromethyl)pyridine-2-thiolato]tin(IV) was also prepared using an electrochemical procedure.^[23]

[Sn(3-CF₃-pyS)₄] (1): $\text{SnCl}_2 \cdot 2\text{H}_2\text{O}$ (0.189 g, 0.84 mmol) was added to a solution of 3-(trifluoromethyl)pyridine-2-thione (0.30 g, 1.67 mmol) and dry triethylamine (0.25 mL, 1.84 mmol) in methanol (20 mL) with constant stirring at room temperature. The solution was evaporated to dryness and the solid was recrystallised from diethyl ether. Yield 38% (0.132 g). $\text{C}_{24}\text{H}_{12}\text{F}_{12}\text{N}_4\text{S}_4\text{Sn}$ (831.4): calcd. C 34.7, H 1.4, N 6.7; found C 34.8, H 1.2, N 6.8. IR (KBr): $\tilde{\nu}$ = 1584, 1563, 1485 cm^{-1} [$\nu(\text{C}=\text{C})$, $\nu(\text{C}=\text{N})$ py]. FAB MS: m/z (%) = 831.6 (1.1) [SnL_4], 654.0 (100) [SnL_3], 475 (9.5) [SnL_2], 298 (27.4) [SnL]. ^1H NMR (CDCl_3 , 300 MHz): δ = 8.15 (d, 1 H, py-H⁶), 7.78 (d, 1 H, py-H⁵), 7.01 (dt, 1 H, py-H⁴) ppm. ^{13}C NMR (CDCl_3 , 300 MHz): δ = 163.1 (py-C²), 124.6 (py-C³), 136.0 (py-C⁴), 121.0 (py-C⁵), 147.2 (py-C⁶), 116.4 (CF_3) ppm. ^{19}F NMR (CDCl_3 , 300 MHz): δ = -65.3 ppm. ^{119}Sn NMR (CDCl_3 , 500 MHz): δ = -662.6 ppm.

[Sn(5-CF₃-pyS)₄] (2): (a) $\text{SnCl}_2 \cdot 2\text{H}_2\text{O}$ (0.189 g, 0.84 mmol) was added to a solution of 5-(trifluoromethyl)pyridine-2-thione (0.30 g, 1.67 mmol) and triethylamine (0.25 mL, 1.84 mmol) in methanol (20 mL) with constant stirring at room temperature. The reaction mixture was stirred for 4 hours and the resulting yellow solid was filtered off, washed with a small amount of diethyl ether, and dried under vacuum. Yield 47% (0.163 g). $\text{C}_{24}\text{H}_{12}\text{F}_{12}\text{N}_4\text{S}_4\text{Sn}$ (831.4): calcd. C 34.7, H 1.4, N 6.7, S 15.4; found C 34.9, H 1.5, N 6.7, S 15.3.

(b) A solution of 5-(trifluoromethyl)pyridine-2-thione (0.267 g, 1.49 mmol) in acetonitrile containing 20 mg of tetraethylammonium perchlorate was electrolysed using a tin rod as the anode and a platinum wire as the cathode. A current of 10 mA was applied during two hours, dissolving 43.39 mg of metal (E_f = 0.49 $\text{mol} \cdot \text{F}^{-1}$). At the end of the electrolytic process the solution was evaporated to dryness and the solid recrystallised from diethyl ether. Yield 69% (0.213 g). $\text{C}_{24}\text{H}_{12}\text{F}_{12}\text{N}_4\text{S}_4\text{Sn}$ (831.4): calcd. C 34.7, H 1.4, N 6.7; found C 34.5, H 1.4, N 6.6. IR (KBr): $\tilde{\nu}$ = 1590, 1540, 1455 cm^{-1} [$\nu(\text{C}=\text{C})$, $\nu(\text{C}=\text{N})$ py]. FAB MS: m/z (%) = 654.0 (100) [SnL_3], 475 (3.5) [SnL_2], 298 (49.7) [SnL]. ^1H NMR (CDCl_3 , 300 MHz): δ = 9.18 (m, 1 H, py-H⁶), 8.51 (m, 1 H, py-H⁴), 7.79 (m, 1 H, py-H³) ppm. ^{13}C NMR (CDCl_3 , 300 MHz): δ = 167.9 (py-C²), 128.6 (py-C³), 134.6 (py-C⁴), 125.0 (py-C⁵), 142.4 (py-C⁶), 121.4 (CF_3) ppm. ^{19}F NMR (CDCl_3 , 300 MHz): δ = -62.7 ppm. ^{119}Sn NMR (CDCl_3 , 500 MHz): δ = -500.5 ppm.

[Pb(3-CF₃-pyS)₂] (3): $\text{Pb}(\text{OAc})_2 \cdot 3\text{H}_2\text{O}$ (0.21 g, 0.55 mmol) was added to a solution of 3-(trifluoromethyl)pyridine-2-thione (0.20 g, 1.11 mmol) and triethylamine (0.17 mL, 1.23 mmol) in methanol (20 mL) with constant stirring at room temperature. The reaction mixture was stirred for 5 hours and the resulting yellow precipitate was filtered off, washed with diethyl ether, and dried under vacuum. The product was recrystallised from diethyl ether. Yield 62% (0.195 g). $\text{C}_{12}\text{H}_6\text{F}_6\text{N}_2\text{PbS}_2$ (563.5): calcd. C 25.6, H 1.1, N 5.0; found C 25.3, H 1.0, N 4.8. IR (KBr): $\tilde{\nu}$ = 1583, 1558, 1442, 1402

cm^{-1} [$\nu(\text{C}=\text{C})$, $\nu(\text{C}=\text{N})$ py]. FAB MS: m/z (%) = 563.8 (4.4) [PbL_2], 385.8 (29.3) [PbL]. ^1H NMR (CDCl_3 , 300 MHz): δ = 8.75 (d, 1 H, py-H⁶), 8.09 (dd, 1 H, py-H⁵), 7.23 (dt, 1 H, py-H⁴) ppm. ^{13}C NMR (CDCl_3 , 300 MHz): δ = 169.9 (py-C²), 128.0 (py-C³), 134.6 (py-C⁴), 121.7 (py-C⁵), 148.4 (py-C⁶), 115.6 (CF_3) ppm. ^{19}F NMR (CDCl_3 , 300 MHz): δ = -48.8 ppm.

[Pb(5-CF₃-pyS)₂] (4): $\text{Pb}(\text{OAc})_2 \cdot 3\text{H}_2\text{O}$ (0.21 g, 0.55 mmol) was added to a solution of 5-(trifluoromethyl)pyridine-2-thione (0.20 g, 1.11 mmol) and triethylamine (0.17 mL, 1.23 mmol) in methanol (20 mL) with constant stirring at room temperature. The reaction mixture was stirred for 5 hours and the resulting yellow precipitate was filtered off, washed with diethyl ether, and dried under vacuum. Yield 18% (0.057 g). $\text{C}_{12}\text{H}_6\text{F}_6\text{N}_2\text{PbS}_2$ (563.5): calcd. C 25.6, H 1.1, N 5.0; found C 25.6, H 1.2, N 5.2. IR (KBr): $\tilde{\nu}$ = 1603, 1547, 1460 cm^{-1} [$\nu(\text{C}=\text{C})$, $\nu(\text{C}=\text{N})$ py]. FAB MS: m/z (%) = 563.8 (0.5) [PbL_2], 385.8 (38.1) [PbL]. ^1H NMR ($[\text{D}_6]\text{DMSO}$, 300 MHz): δ = 8.38 (d, 1 H, py-H⁶), 7.46 (dd, 1 H, py-H⁴), 6.87 (dd, 1 H, py-H³) ppm. ^{13}C NMR (CDCl_3 , 300 MHz): δ = 176.9 (py-C²), 131.9 (py-C⁴), 130.3 (py-C⁵), 142.1 (py-C⁶), 117.6 (CF_3) ppm. ^{19}F NMR (CDCl_3 , 300 MHz): δ = -56.2 ppm.

In the cases of compounds **1**, **2**, and **3**, X-ray quality crystals were obtained from saturated solutions of the complexes by slow evaporation of the solvents at room temperature.

X-ray Crystal Structure Determinations

Data Collection and Processing: X-ray data were collected on a Smart-CCD-1000 Bruker diffractometer for **1** and on an Enraf–Nonius CAD4 diffractometer for **2** and **3**; both fitted with graphite monochromated Mo-K_α radiation (λ = 0.71073 Å). The data were collected at 293 K for all structures. The ω -scan technique was employed to measure intensities in all crystals up to a maximum Bragg angle of 26.37° for **1**, 24.97° for **2**, and 28.04° for **3**. Decomposition of the crystals did not occur during data collection. Corrections were applied for Lorentz and polarisation effects and for absorption (μ = 1.195 mm^{-1} for **1**, 1.223 mm^{-1} for **2**, and 11.683 mm^{-1} for **3**).^[24] A total of 14630 reflections for **1**, 4014 for **2**, and 3652 for **3** were collected, of which 1569 reflections in **1**, 3829 in **2**, and 3585 in **3** were unique [R_{int} = 0.0362 (**1**), 0.0148 (**2**), 0.0766 (**3**)] and, of these, 1261 (**1**), 3829 (**2**), and 1515 (**3**) satisfied the $I > 2\sigma(I)$ criterion of observability and were used in the subsequent analysis.

Structure Analysis and Refinement: The structures were solved by direct methods and missing atoms were located in the difference Fourier map and included in subsequent refinement cycles. The structures were refined by full-matrix least-squares refinement on F^2 , using anisotropic displacement parameters for all non-hydrogen atoms. In all cases, hydrogen atoms were included using a riding model with C–H distances of 0.93–0.97 Å and fixed isotropic thermal parameters, except for **2**, where hydrogen atoms were located in the difference Fourier map and refined isotropically. A weighting scheme of the form $\omega = 1/\sigma^2(F)$ was introduced and the refinement proceeded smoothly to convergence with a maximum δ/σ = 0.000 when R = 0.0270, R_w = 0.0597 and GOF = 1.092 (goodness-of-fit) for 102 variables for **1**, maximum δ/σ = 0.001 when R = 0.0306, R_w = 0.0861 and GOF = 1.045 for 491 variables for **2** and δ/σ = 0.001 when R = 0.1145, R_w = 0.2843 and GOF = 1.049 for 208 variables for **3**. The residual analysis of the variance showed no special features and the maximum and minimum residual electron density peaks in the final difference map were, respectively, +0.24 and -0.23 $\text{e} \cdot \text{\AA}^{-3}$ in **1**, +0.64 and -0.45 $\text{e} \cdot \text{\AA}^{-3}$ in **2**, and +4.84 and -4.40 $\text{e} \cdot \text{\AA}^{-3}$ in **3**.

Table 5. Crystal data and experimental details for **1**, **2** and **3**

	1	2	3
Empirical formula	C ₆ H ₃ F ₃ NSSn _{0.25}	C ₂₄ H ₁₂ F ₁₂ N ₄ S ₄ Sn	C ₁₂ H ₆ F ₆ N ₂ PbS ₂
Molecular weight	207.83	831.30	563.50
Temperature [K]	293(2)	293(2)	293(2)
Wavelength [Å]	0.71073	0.71073	0.71073
Crystal System	Tetragonal	Triclinic	Monoclinic
Space group	<i>I</i> 4(1)/a	<i>P</i> – 1	<i>C</i> 2/c
<i>a</i> [Å]	13.7103(18)	11.9010(10)	27.45(5)
<i>b</i> [Å]	13.7103(18)	12.554(2)	4.458(1)
<i>c</i> [Å]	16.418(3)	12.794(2)	24.325(6)
α [deg]	90	99.910(10)	90
β [deg]	90	117.080(10)	91.90(6)
γ [deg]	90	107.770(10)	90
Cell volume [Å ³]	3086.1(8)	1507.7(4)	2975(6)
<i>Z</i>	4	2	8
<i>D_c</i> [Mg·m ^{–3}]	1.789	1.831	2.516
$\lambda(\text{Mo-}K_{\alpha})$ [mm ^{–1}]	1.195	1.223	11.683
Crystal size [mm]	0.49 × 0.38 × 0.30	0.40 × 0.25 × 0.18	0.32 × 0.32 × 0.08
θ limits [deg]	1.94–26.37	1.83–24.97	4.41–28.04
Collected reflections	14630	4014	3652
Unique reflections	1569 [<i>R</i> _{int} = 0.0362]	3829 [<i>R</i> _{int} = 0.0148]	3585 [<i>R</i> _{int} = 0.0766]
Observed reflections	1261	3829	1515
[<i>F</i> _o > 2σ(<i>F</i> _o)]			
Parameters	102	491	208
Goodness of fit on <i>F</i> ²	1.092	1.045	1.049
<i>R</i> 1(<i>F</i>) ^[a]	0.0270	0.0306	0.1145
<i>wR</i> 2(<i>F</i> ²) ^[b]	0.0597	0.0861	0.2843
Largest difference peak and hole [e·Å ^{–3}]	0.24 and –0.23	0.64 and –0.45	4.84 and –4.40

^[a] $R1 = [|F_o| - |F_c|]/|F_o|$. ^[b] $wR2 = [(F_o^2 - F_c^2)/(F_o^2)]^{1/2}$ where $w = 1/[\sigma^2(F_o^2) + (aP)^2 + bP]$ and $P = (F_o^2 + 2F_c^2)/3$.

The crystallographic programs in SHELX97^[25] were used for the structure solutions and refinement. Atomic scattering factors and anomalous-dispersion corrections for all atoms were taken from the International Tables for X-ray Crystallography.^[26] Crystallographic data for these compounds are given in Table 5. Ortep3^[27] drawings with the numbering scheme used are shown in Figures 1, 3, and 4.

CCDC-186656 (**1**), -186658 (**2**), and -186657 (**3**) contain the supplementary crystallographic data for this paper. These data can be obtained free of charge at www.ccdc.cam.ac.uk/conts/retrieving.html [or from the Cambridge Crystallographic Data Centre, 12, Union Road, Cambridge CB2 1EZ, UK; Fax: (internat.) +44-1223/336-033; E-mail: deposit@ccdc.cam.ac.uk].

Acknowledgments

We thank the Xunta de Galicia (PGIDT00PXI20305PR) for financial support. One of us (A. S.-P.) thanks Ministerio de Educación y Cultura (Spain) for a doctoral grant.

- ^[1] E. S. Raper, *Coord. Chem. Rev.* **1985**, *61*, 115–184; E. S. Raper, *Coord. Chem. Rev.* **1996**, *153*, 199–255; E. S. Raper, *Coord. Chem. Rev.* **1997**, *165*, 475–567.
^[2] B. Krebs, G. Henkel, *Angew. Chem. Int. Ed. Engl.* **1991**, *30*, 769–788.
^[3] ^[3a] I. G. Dance, *Polyhedron* **1986**, *5*, 1037–1104. ^[3b] P. G. Blower, J. R. Dilworth, *Coord. Chem. Rev.* **1987**, *76*, 121–185. ^[3c] J. R. Dilworth, J. Hu, *Adv. Inorg. Chem.* **1993**, *40*, 411–459.
^[4] E. J. Fernández, M. B. Hurthouse, M. Laguna, R. Terrota, *J. Organomet. Chem.* **1999**, *574*, 207–212; S. R. Foley, G. P. A. Yap, D. S. Richeson, *J. Chem. Soc., Dalton Trans.* **2000**, 1663–1668; R. Jurkschat, V. Pieper, S. Seemeyer, M. Schürmann, M. Biesmans, I. Verbruggen, R. Willem, *Organometallics*

- 2001**, *20*, 868–880; D. Dakternieks, K. Jurkschat, R. Tozer, J. Hook, E. R. S. Tickink, *Organometallics* **1997**, *16*, 3696–3706.
^[5] E. Block, G. Ofori-Okai, J. Zubieta, *J. Am. Chem. Soc.* **1989**, *111*, 2327–2329.
^[6] M. M. Jones, *Met. Ions Biol. Syst.* **1983**, *16*, 47–83.
^[7] L. C. Damude, P. A. W. Dean, V. Masivannan, R. S. Srivastava, J. J. Vitali, *Can. J. Chem.* **1990**, *68*, 1323–1331.
^[8] E. Block, G. Ofori-Okai, H. Hang, J. Wu, J. Zubieta, *Inorg. Chim. Acta* **1991**, *190*, 5–6.
^[9] E. Labisbal, A. de Blas, J. A. García-Vázquez, J. Romero, M. L. Durán, A. Sousa, N. A. Bailey, D. E. Fenton, P. B. Leeson, R. V. Parish, *Polyhedron* **1992**, *11*, 227–233; E. Labisbal, J. A. García-Vázquez, J. Romero, A. Sousa, A. Castiñeiras, C. Maichle-Mössmer, U. Russo, *Inorg. Chim. Acta* **1994**, *223*, 87–92.
^[10] S. W. Ng, C. Wei, V. G. K. Das, T. C. W. Mak, *J. Organomet. Chem.* **1987**, *334*, 295–305.
^[11] C. S. Harreld, E. O. Schlemper, *Acta Crystallogr., Sect. B* **1971**, *27*, 1964–1969.
^[12] J. Potenza, R. J. Johnson, D. Mastropaolo, *Acta Crystallogr., Sect. B* **1976**, *32*, 941–943.
^[13] B. R. Penfold, *Acta Crystallogr.* **1953**, *6*, 707–713.
^[14] J. A. García-Vázquez, J. Romero, A. Sousa-Pedrares, M. L. Louro, A. Sousa, J. Zubieta, *J. Chem. Soc., Dalton Trans.* **2000**, 559–567.
^[15] A. W. Addison, T. N. Rao, J. Reedijk, J. Van Rijn, G. N. Verschoor, *J. Chem. Dalton Trans.* **1984**, 1349–1356.
^[16] K. Abu-Dari, T. B. Karpinshin, K. N. Raymond, *Inorg. Chem.* **1993**, *32*, 3052–3055.
^[17] N. A. Bailey, D. E. Fenton, I. T. Jackson, R. Moody, C. R. de Barbarin, *J. Chem. Soc., Chem. Commun.* **1983**, 1463–1465; L. M. Engelhardt, J. M. Patrick, C. R. Whitaker, A. H. White, *Aust. J. Chem.* **1987**, *40*, 2107–2114.
^[18] R. V. Parish, *Prog. Inorg. Chem.* **1972**, *15*, 101.
^[19] P. A. Flinn, in: *Mössbauer Isomer Shifts* (Eds.: G. K. Shenoy, T. E. Wagner), Elsevier, North-Holland, **1978**, pp. 593–616.

- [²⁰] J. Silver, in: *Solid State Organometallic Chemistry: Methods and Applications* (Eds.: M. Gielen, R. Willem, B. Wrackmeyer), John Wiley and Sons Ltd, **1999**, pp. 279–396.
- [²¹] R. V. Parish, R. H. Platt, *Inorg. Chim. Acta* **1970**, *4*, 65.
- [²²] J. Ovenstone, P. J. Titler, R. Withnall, J. Silver, *J. Phys. Chem. B* **2001**, *105*, 7170–7177.
- [²³] J. A. García-Vázquez, J. Romero, A. Sousa, *Coord. Chem. Rev.* **1999**, *193–195*, 691.
- [²⁴] N. Walker, D. Stuart, *Acta Crystallogr., Sect. A* **1983**, *39*, 158–166.
- [²⁵] *SHELX97* [Includes SHELXS-97, SHELXL-97, CIFTAB] – Programs for Crystal Structure Analysis (Release 97–2). G. M. Sheldrick, Institut für Anorganische Chemie der Universität, Tammanstrasse 4, 3400 Göttingen, Germany, **1998**.
- [²⁶] *International Tables for Crystallography, Volume C* (Ed.: A. J. C. Wilson), Kluwer Academic Publishers, Dordrecht, The Netherlands, **1995**.
- [²⁷] ORTEP3 for Windows: L. J. Farrugia, *J. Appl. Crystallogr.* **1997**, *30*, 565.

Received June 25, 2002

[I02349]